Tetrahedron 65 (2009) 4540–4546

Contents lists available at ScienceDirect

Tetrahedron

journal homepage: www.elsevier.com/locate/tet

A modular ligand design for cation sensors: phosphorus-supported pyrene-containing ligands as efficient Cu(II) and Mg(II) sensors

Vadapalli Chandrasekhar [a,*], Mrituanjay D. Pandey [a], Prasenjit Bag [a], Siddharth Pandey [b]

[a] Department of Chemistry, Indian Institute of Technology, Kanpur 208016, India
[b] Department of Chemistry, Indian Institute of Technology Delhi, Hauz Khas, New Delhi 110016, India

ARTICLE INFO

Article history:
Received 25 December 2008
Received in revised form 28 March 2009
Accepted 30 March 2009
Available online 5 April 2009

Keywords:
Phosphorus
Pyrene
Fluorescence
X-ray crystallography

ABSTRACT

A modular ligand design allowed the assembly of four phosphorus-supported pyrene-containing ligands. The number of pyrene arms could be varied from 1 to 6 depending on the phosphorus support. While ligands containing one and three pyrene arms are excellent fluorescence-based sensors of Cu^{2+}, the ligand containing two pyrene arms shows a high specificity for Mg^{2+}.

1. Introduction

In recent years there has been considerable research interest in the area of molecular sensors, which can detect cations (or anions) with a high degree of specificity even at low concentrations.[1–5] Detection techniques based on optical spectroscopic methods have been favoured in view of the simplicity of the technique as well as rapid nature of detection. In general the design of ligands is carried out with a view to induce absorption spectral changes or fluorescence emission changes upon interaction with cations.[6–8] Fluorescence-based methods are more sensitive than the corresponding absorption techniques and hence there has been considerable interest in the design of new ligands that would show significant changes in their fluorescence output upon interaction with a cation input.[9–15] We have been interested in phosphorus-based ligands for some time in view of their modular design and also because the latter allows ready assembly of a wide choice of ligands with varying properties. For example, using (*S*)P[N(Me)N=CH–C_6H_4–2-OH]$_3$ we were able to assemble neutral trinuclear derivatives (L_2M_3) whereas by the use of (*S*)P[N(Me)N=CHC_6H_4–2-OH–3-OMe]$_3$ we could prepare ionic 3d–4f assemblies possessing interesting magnetic properties including single molecule magnet behaviour.[16,17] In view of this versatility it was of interest to probe if this design allowed the preparation of ligands whose fluorescence properties could be affected by metalation. Our particular interest was the possibility of finding an effective fluorescence-based sensor for Cu^{2+} in view of the fact that paramagnetic ions quench fluorescence[18–21] and only in some instances a fluorescence enhancement has been observed.[22–26] Accordingly, we report herein, the design, assembly and structural characterization of a family of phosphorus-supported pyrene containing ligands $Ph_2P(O)[N(Me)N{=}CH(Py)]$ (**1**), PhP(O)[N(Me)N=CH(Py)]$_2$ (**2**), (*S*)P[N(Me)N=CH-Py]$_3$ (**3**) and N_3P_3[N(Me)N=CH-Py]$_6$ (**4**) (Py=1-pyrenyl). While **1** and **3** are excellent sensors of Cu^{2+}, **2** is specific for Mg^{2+}.

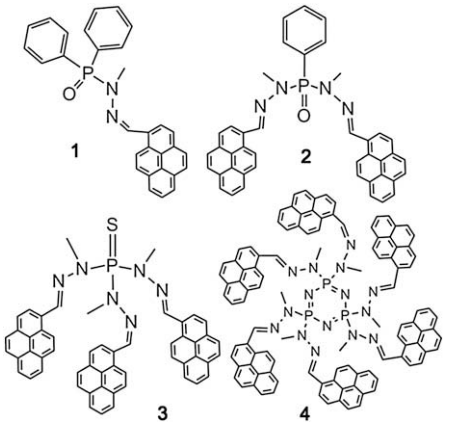

Figure 1. Phosphorus-supported pyrene-containing ligands **1**–**4**.

* Corresponding author.
E-mail address: vc@iitk.ac.in (V. Chandrasekhar).

0040-4020/$ – see front matter © 2009 Elsevier Ltd. All rights reserved.
doi:10.1016/j.tet.2009.03.098

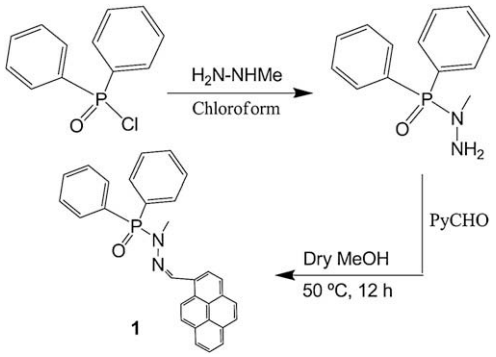

Scheme 1. Synthesis of **1**.

2. Results and discussion

The synthesis of the ligands **1**–**4** was carried out by a two-step protocol and involved the conversion of the chloro precursors into the corresponding phosphorus hydrazides by a regiospecific reaction with *N*-methylhydrazine. Condensation of the hydrazides with pyrene-1-carboxaldehyde afforded **1**–**4** in excellent yields (Fig. 1). A representative synthetic protocol is shown in Scheme 1. The conversion of the chloro precursors into the products is readily monitored by $^{31}P\{H\}$ NMR [cf. δ (^{31}P); (*S*)PCl_3 31.7 (s); (*S*)$P[N(Me)NH_2]_3$, 84.5 (s); **3**, 75.1 (s)]. Compounds **1**–**4** are soluble in a wide range of organic solvents. The chemical integrity of these compounds is retained in solution as evidenced by the presence of strong $[M+H]^+$ peaks in their ESI-MS spectra recorded under positive ion mode (see Supplementary data). Finally, **1**–**3** were also characterized by solid state X-ray crystallography. Compound **2** crystallized in two modifications, one as a methanol solvate and the other without any solvent of crystallization. The perspective views

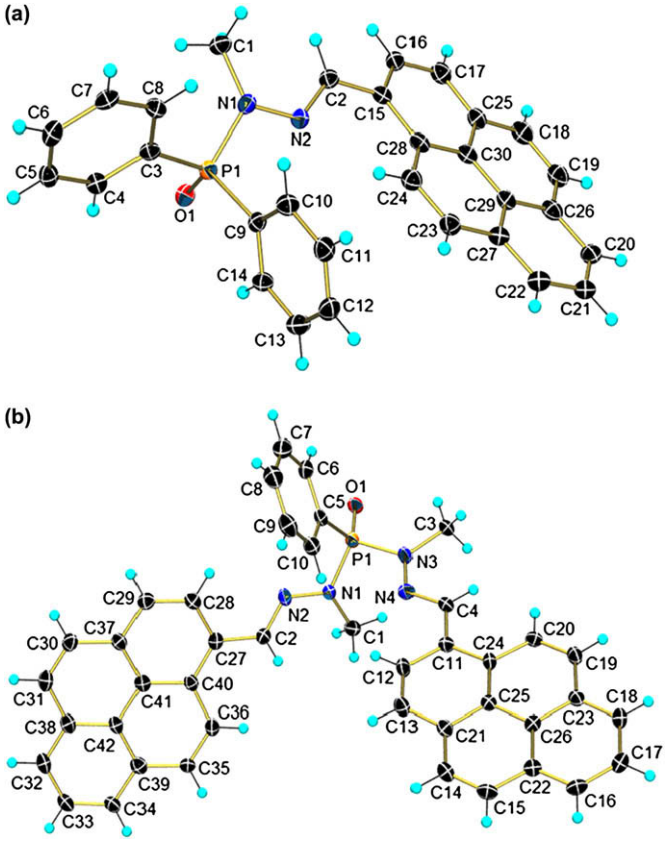

Figure 2. ORTEP diagrams of **1** (a) and **2**·MeOH (b) with 50% thermal ellipsoids (solvent molecules are omitted for clarity). Selected bond distances (Å) and angles (°) are as follows: **1**: C(3)–P(1), 1.803(3); C(9)–P(1), 1.800(2); N(1)–P(1), 1.687(2); P(1)–O(1), 1.4797(19); O(1)–P(1)–N(1), 116.69(11); O(1)–P(1)–C(9), 113.36(11); N(1)–P(1)–C(9), 103.21(11); O(1)–P(1)–C(3), 110.99(11); N(1)–P(1)–C(3), 104.47(11); C(9)–P(1)–C(3), 107.27(11). **2**·MeOH: C(5)–P(1), 1.787(3); N(1)–P(1), 1.663(3); N(3)–P(1), 1.669(2); O(1)–P(1), 1.472(2); O(1)–P(1)–N(1), 116.56(12); O(1)–P(1)–N(3), 108.88(12); N(1)–P(1)–N(3), 102.65(12); O(1)–P(1)–C(5), 112.49(13); N(1)–P(1)–C(5), 105.63(13); N(3)–P(1)–C(5), 110.12(13).

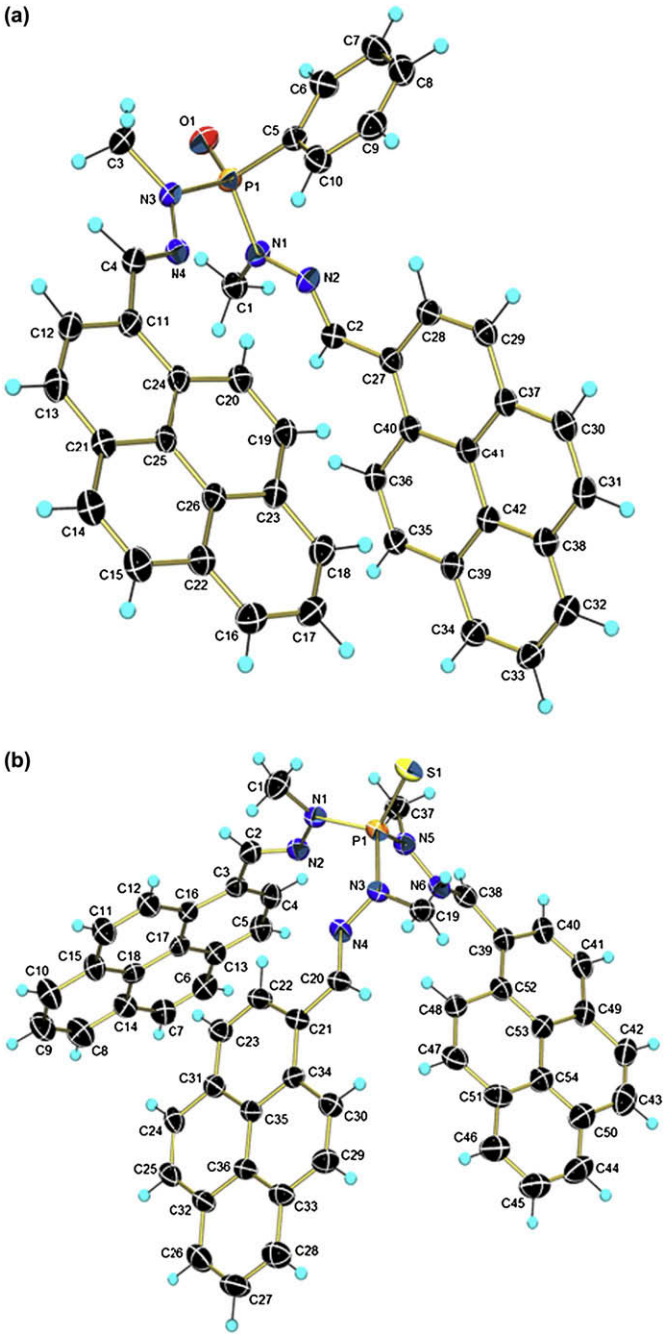

Figure 3. ORTEP diagrams of **2** (a) and **3** (b) with 50% and 30% thermal ellipsoids, respectively. Selected bond distances (Å) and angles (°) are as follows: **2**: C(5)–P(1), 1.788(2); N(1)–P(1), 1.6603(19); N(3)–P(1), 1.678(2); P(1)–O(1), 1.4696(16); O(1)–P(1)–N(1), 112.42(10); O(1)–P(1)–N(3), 108.65(10); N(1)–P(1)–N(3), 107.87(10); O(1)–P(1)–C(5), 113.77(10); N(1)–P(1)–C(5), 105.96(10); N(3)–P(1)–C(5), 107.92(11). **3**: N(1)–P(1), 1.659(4); N(3)–P(1), 1.667(4); N(5)–P(1), 1.672(4); P(1)–S(1), 1.9247(19); N(1)–P(1)–N(3), 107.9(2); N(1)–P(1)–N(5), 101.7(2); N(3)–P(1)–N(5), 106.3(2); N(1)–P(1)–S(1), 112.54(16); N(3)–P(1)–S(1), 110.37(15); N(5)–P(1)–S(1), 117.32(15).

Table 1
Crystallographic data and structure refinement details for **1**, **2**, **2**·MeOH and **3**

	1	**2**	**2**·MeOH	**3**
Empirical formula	$C_{36}H_{29}N_2OP$	$C_{42}H_{31}N_4OP$	$C_{43}H_{35}N_4O_2P$	$C_{54}H_{39}N_6PS$
Formula weight	536.58	638.68	670.72	834.94
Temperature (K)	153(2)	100(2)	100(2)	273(2)
Wavelength (Å)	0.71073	0.71073	0.71073	0.71073
Crystal system	Triclinic	Monoclinic	Triclinic	Triclinic
Space group	*P*-1	*P*21/*n*	*P*-1	*P*-1
Unit cell	*a*=8.4772(11)	*a*=10.0285(7)	*a*=6.792	*a*=10.385(5)
dimensions (Å), (°)	*b*=10.2534(13)	*b*=11.8695(9)	*b*=15.720	*b*=13.784(7)
	c=17.442(2)	*c*=26.634(2)	*c*=16.618	*c*=15.118(8)
	α=77.418(2)	*α*=90	*α*=75.52	*α*=86.293(10)
	β=88.766(2)	*β*=99.1170(10)	*β*=89.65	*β*=76.600(11)
	γ=65.632(2)	*γ*=90	*γ*=78.57	*γ*=89.766(10)
Volume (Å^3)	1343.9(3)	3130.3(4)	1682.1	2100.6(19)
Z, D_{calcd} [Mg/m^3]	2, 1.326	4, 1.355	2, 1.324	2, 1.320
μ [mm^{-1}]	0.136	0.131	0.127	0.162
F(000)	564	1336	704	872
Crystal size (mm^3)	0.11×0.09×0.06	0.08×0.05×0.03	0.103×0.072×0.047	0.087×0.072×0.057
θ Range (°)	2.29–27.00	2.08–27.00	2.09–26.50	2.02–25.00
Index ranges	−10≤*h*≤10	−12≤*h*≤12	−8≤*h*≤8	−9≤*h*≤12
	−13≤*k*≤13	−15≤*k*≤11	−17≤*k*≤19	−15≤*k*≤16
	−22≤*l*≤11	−34≤*l*≤33	−19≤*l*≤20	−14≤*l*≤17
Reflections collected	8130	18 465	9914	10 791
Independent reflections	5683 [*R*(int)=0.0261]	6803 [*R*(int)=0.0434]	6795 [*R*(int)=0.0277]	7261 [*R*(int)=0.0480]
Data/restraints/parameters	5683/0/362	6803/0/557	6795/0/455	7261/0/562
Goodness-of-fit on F^2	1.059	1.062	1.018	0.954
Final *R* indices [*I*>2sigma(*I*)]	*R*1=0.064	*R*1=0.0544	*R*1=0.0658	*R*1=0.0702
	*wR*2=0.1802	*wR*2=0.1247	*wR*2=0.1650	*wR*2=0.1557
R indices (all data)	*R*1=0.0835	*R*1=0.0800	*R*1=0.0990	*R*1=0.1719
	*wR*2=0.2450	*wR*2=0.1513	*wR*2=0.2143	*wR*2=0.2260
Largest diff. peak and hole (e Å^{-3})	0.803 and −0.663	0.379 and −0.358	0.633 and −0.358	0.356 and −0.329

of molecular structures are given in Figures 2 and 3. Selected internuclear distances and bond angles are included in figure captions. Crystal and cell parameter data for **1**, **2**, **2**·MeOH and **3** are given in Table 1. **1**, **2**·MeOH and **3** crystallize in the triclinic space group *P*-1 (No. 2) while **2** crystallizes in the monoclinic space group $P2_1/n$ (No. 14). The molecular structures of all the compounds reveal a central tetrahedral phosphorus atom, which acts as a support to hold the multi-site coordination platform built around it. The P–O bond distances observed in **1** and **2** are 1.4797(19) Å and 1.4696(16) Å, respectively, which is consistent with P═O distances found in literature.[27a] The P–N bond distances in **1**, **2** and **3** are 1.687(2) Å, 1.678(2) Å and 1.672(4) Å, respectively. This may be compared with the P–N single bond distance (observed in P(V) compounds), which is 1.70 Å.[27b] The crystal packing of **1**–**3** shows a rich supramolecular chemistry as a result of intra- and intermolecular CH···π and π···π interactions (Fig. 4). Supramolecular self-assembly in compounds **1**, **2**·MeOH and **2** appears to be effected by the molecular association through C–H···O hydrogen bonds (Fig. 5). Hydrogen bond parameters for these compounds are given in Table 2.

The absorption spectra of **1**–**4** in toluene/acetonitrile (10:1, v/v) are characterized by peaks both at high and low energy. It is

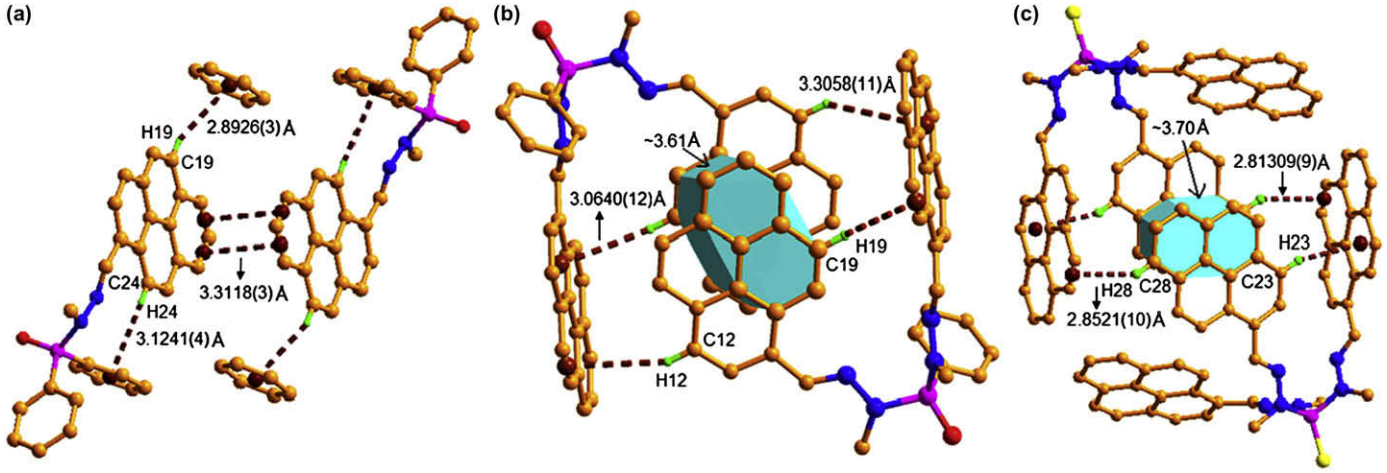

Figure 4. Interplay of intra- and intermolecular CH···π and π···π interactions of **1** (a), **2** (b) and **3** (c) showing supramolecular architecture. Colour code: orange, carbon; blue, nitrogen; red, oxygen; pink, phosphorus; yellow, sulfur.

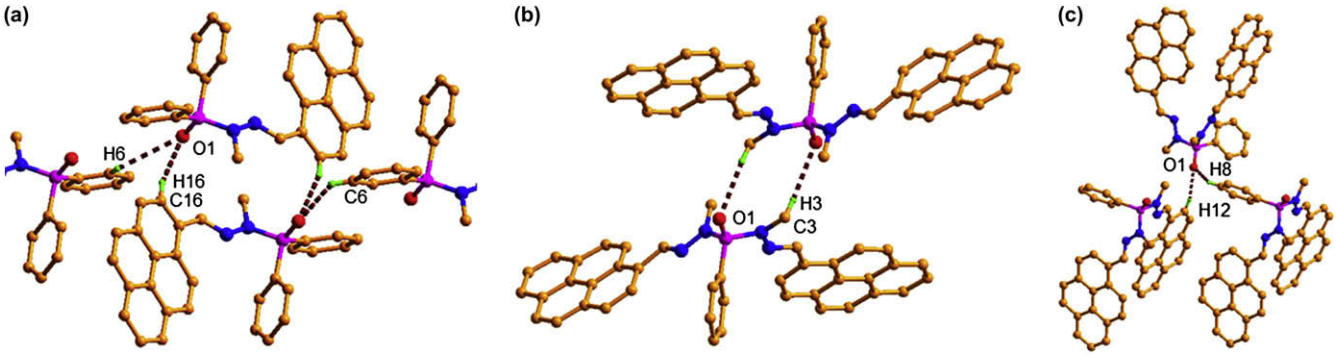

Figure 5. Formation of chain in **1** (a), **2**·MeOH (b) and **2** (c) via intermolecular hydrogen bonding.

Table 2
Hydrogen bond parameters

Compounds	D–H···A	*d*(D–H) Å	*d*(H···A) Å	*d*(D···A) Å	∠(DHA) °	Symmetry[i]
1	C6–H6···O1[i]	0.93	2.4388 (17)	3.2734 (33)	149.398 (181)	(x, $-1+y$, z)
	C16–H16···O1[i]	0.93	2.6178 (17)	3.5172 (33)	163.079 (172)	(x, $-1+y$, z)
2·MeOH	C3–H3C···O1[i]	0.96	2.7111 (20)	3.6077 (36)	155.635 (181)	($2-x$, $2-y$, $-z$)
2	C8–H8···O1[i]	0.98	2.4037 (246)	3.2065 (31)	138.454 (2010)	($1.5-x$, $1/2+y$, $1/2-z$)
	C12–H12···O1[i]	0.95	2.3796 (233)	3.2994 (28)	163.408 (1969)	($2.5-x$, $1/2+y$, $1/2-z$)

interesting to note that while the λ_{max} values of all the four ligands are nearly invariant, their absorbance values increase as the number of pyrene arms is increased [cf. **1**, λ_{max} (ε); 286 (15 200), 295 (17 700), 365 (30 000), 380 (27 000)] (Fig. 6A). These spectra are typical for pyrene-containing compounds and the absorptions are due to pyrene π–π^* transition.[27–32]

Compounds **1**–**4** show an emission around 410 nm upon excitation at 363 nm. A few low energy bands are also seen in the emission spectra. Similar to the absorbance values, the fluorescence intensity also increases as the number of pyrene units is increased from one to six (Fig. 6B).

Although interaction of **1**–**4** with various metal ions (Ca^{2+}, Cd^{2+}, Cu^{2+}, Li^{+}, Mg^{2+}, Na^{+}, Ni^{2+}, Zn^{2+}) causes slight changes in the absorption spectra including the appearance of new d–d bands (see Supplementary data) clear and specific effects that can be used as unique detection features for individual metal ions are not discerned (Fig. 7). This situation, however, changes quite dramatically in the fluorescence spectra (Fig. 8). Interaction of **1** with various metal salts reveals that only Cu^{2+} effects a significant fluorescence enhancement as revealed by a fluorescence enhancement factor (FEF) of 5.7. The latter was measured with respect to the fluorescence intensity. It must be mentioned that FEFs calculated w.r.t. quantum yields[33] also show a similar trend as those found with just fluorescence intensities. The fluorescence enhancement on interaction of **1**–**3** with metal ions seems to depend on the efficiency of binding. Thus **1** and **3** bind Cu^{2+} more effectively (4.7×10^4 and 3.1×10^5 M^{-1}) while **2** binds to Mg^{2+} very strongly[34,35] (1.97×10^5 M^{-1}) (Table 3). The fluorescence band, however, does not experience any significant shift. The maximum FEF obtained for Cu^{2+} with **1** occurs at an L:M ratio of 1:10. Further addition of Cu^{2+} does not change the FEF. Similar to **1**, the ligand with three pyrene arms also is sensitive Cu^{2+}, only more so. An FEF of 9.5 is observed in this case. Interestingly, addition of other metal salts (100.0 μM) to a solution containing **1** or **3** (10.0 μM) and Cu^{2+} (50.0 μM) ions does not affect the fluorescence behaviour indicating that these ligands can effectively sense Cu^{2+} even in the presence of other metal ions similarly to what was reported previously.[36] Ligand **2** containing two pyrene arms, in contrast to **1** and **3**, is sensitive specifically to Mg^{2+} ions with a very high FEF of 15.5 (Fig. 9).

The mechanism of fluorescence enhancement of **1**, **2** and **3** upon interaction with metal ions seems to lie in an inhibition of a photoinduced electron transfer (PET) process[37–40] (Scheme 2). Thus, the engagement of the lone pairs of nitrogen atoms in coordination prevents their utilization in a PET-type quenching process. Compound **4** containing six pyrene arms is ineffective in binding to metal ions presumably because of steric effects.

3. Conclusions

In summary we report a modular design of phosphorus-supported multi-pyrene ligands. Changing the number of pyrene arms modulates the specificity of metal ion recognition.

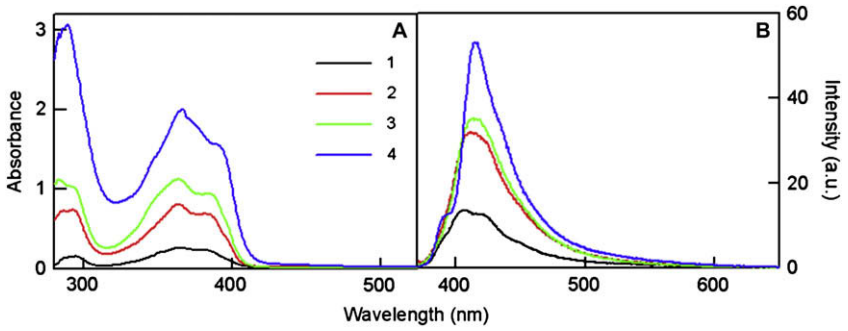

Figure 6. (A) UV–vis and (B) fluorescence spectra of **1**–**4** (10 μM) in toluene/acetonitrile (10:1, v/v).

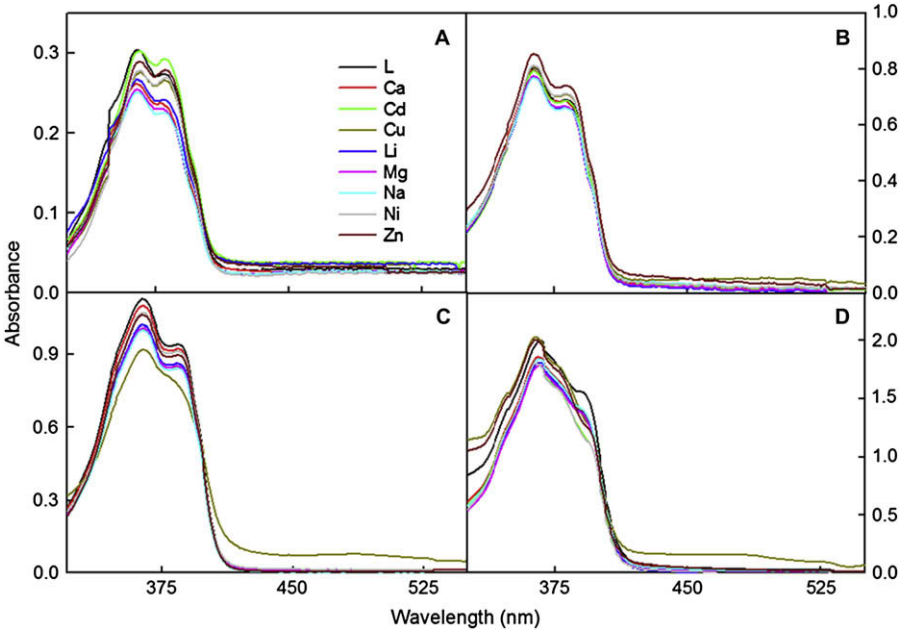

Figure 7. Absorption spectra of pure ligands, **1** (A), **2** (B), **3** (C) and **4** (D) (10.0 μM) and after addition of metal perchlorates (100.0 μM) in acetonitrile/toluene (1:10).

4. Experimental

4.1. General

All fluorescence and absorption spectra were recorded on a Varian Luminescence Cary eclipsed and CARY win 100 Bio UV–vis spectrophotometer with a 10 mm quartz cell at 25±0.1 °C. Melting points were measured using a JSGW melting point apparatus and are uncorrected. ^{1}H NMR spectra were obtained on a JEOL-JNM LAMBDA 400 model spectrometer operating at 400.0 MHz. ^{1}H and ^{31}P NMR spectra were also obtained in $CDCl_3$ solutions on a JEOL-DELTA2 500 model spectrometer operating at 500 and 202.5 MHz, respectively. The chemical shifts are referenced with respect to TMS for ^{1}H and 85% H_3PO_4 for ^{31}P NMR. ESI-HRMS mass spectra were recorded on a MICROMASS QUATTRO II triple quadrupole mass spectrometer. The ESI capillary was set at 3.5 kV and the cone voltage was 40 V. The crystal data for the compounds **1**, **2** and **3** were collected on a Bruker SMART APEX CCD Diffractometer. The program *SMART* (version 6.45) was used for collecting frames of data, indexing reflections and determining lattice parameters. *SAINT* was used for integration of the intensity of reflections and scaling. The program *SADABS* was used for absorption correction.

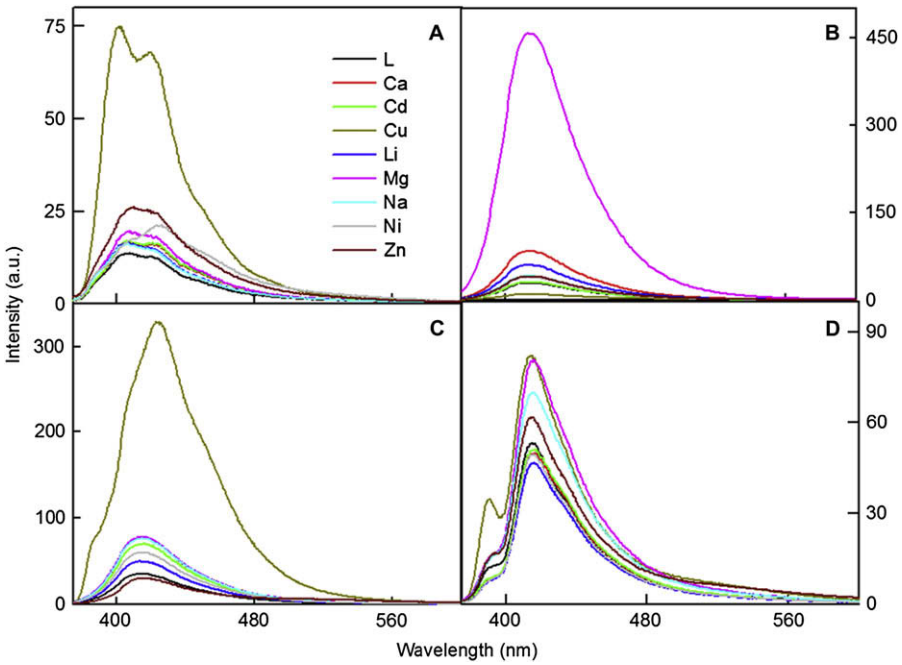

Figure 8. Fluorescence spectra of **1** (A), **2** (B), **3** (C) and **4** (D) (10.0 μM) and after addition of 10 equiv of various metal ions in acetonitrile/toluene (1:10). An excitation wavelength of 363 nm was employed.

Table 3
Spectroscopic data of **1**–**4** upon addition of metal ions

Compounds	λ_{max}, nm (ε)	λ_{em}, nm	Φ_F	K_a, M^{-1}
1	286 (1.52×10^4), 295 (1.77×10^4), 365 (3.0×10^4), 380 (2.7×10^4)	410, 420	0.0035	—
2	284 (7.2×10^4), 293 (7.5×10^4), 364 (8.19×10^4), 382 (6.95×10^4)	414	0.0047	—
3	283 (1.12×10^5), 295 (1.02×10^5), 362 (1.45×10^5), 386 (9.24×10^4)	413	0.0050	—
4	284 (2.91×10^5), 290 (3.08×10^5), 366 (2.01×10^5), 388 (1.56×10^5)	392, 414	0.0052	
1+Cu(II)	286, 295, 365, 380, 490	402, 418	0.046	4.7×10^4
2+Cu(II)	284, 293, 364, 382	413	0.005	2.4×10^4
3+Cu(II)	283, 295, 362, 386, 490	423	0.068	3.1×10^5
4+Cu(II)	284, 290, 366, 388, 490	391, 414	0.0053	1.57×10^4
1+Mg(II)	292, 364, 377	407, 423	0.004	2.6×10^4
2+Mg(II)	291, 363, 382	413	0.070	1.97×10^5
3+Mg(II)	287, 293, 363, 384	415	0.006	2.1×10^4
4+Mg(II)	288, 364, 391	392, 416	0.005	1.79×10^4

The crystal structures were solved and refined by full matrix least-squares methods against F^2 by using the program *SHELXTL*-97.[41] All non-hydrogen atoms were refined with anisotropic displacement parameters. Hydrogen positions were fixed at calculated positions and refined isotropically. The figures are generated by using *Diamond 3.1e* programme. Ph_2POCl, $PhPOCl_2$, $N_3P_3Cl_6$, pyrene-1-carboxaldehyde and metal salts $Cu(ClO_4)_2$, $LiClO_4$ and $NaClO_4$, were purchased from Aldrich. $Zn(ClO_4)_2$, $Cd(ClO_4)_2$, $Ni(ClO_4)_2$, $Mg(ClO_4)_2$, $Ca(ClO_4)_2$ were prepared from their carbonate salts by a reaction with perchloric acid. (*S*)PCl_3 was purchased from Fluka (Switzerland). *N*-Methylhydrazine was obtained as a gift from the Vikram Sarabhai Space Research Centre, Thiruvananthapuram, India. Solvents were purchased from S.D. Fine Chemicals (India) and they were purified prior to use.

4.2. General titration procedure of the ligands with metal ions

A 1.0×10^{-5} M stock solutions of **1**–**4** were prepared in acetonitrile/toluene (1:10). Metal ion stock solutions were prepared in acetonitrile keeping a concentration of 2.0×10^{-3} M. The titration procedure of the ligands with metal ions was as follows. A 2 mL solution of the ligand was filled in a quartz cell of 1 cm optical path length. 100.0 μL of the stock solution of the metal ion was added into the quartz cell gradually by using a micro-pipette, in order to maintain the total volume of testing solution without obvious change. All titrations were carried out at room temperature. For the fluorescence spectra the excitation wavelength was kept at 363 nm.

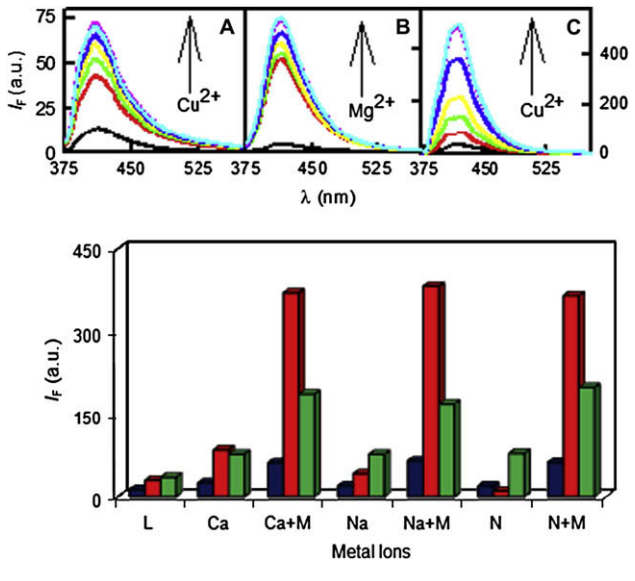

Figure 9. Fluorescence spectra (λ_{ext}=363 nm) of **1**–**3** (graphs A–C) (10.0 μM) at room temperature upon the addition of increasing amounts of metal ions; colour code: 0 (black), 20.0 (red), 40.0 (green), 60.0 (yellow), 80.0 (blue), 100.0 (pink) and 120.0 μm (cyan). (D) Representation of fluorescence spectra in Tabular form **1** (blue), **2** (red) and **3** (green) in the presence of other cations. For **1** and **3**, M=Cu, N=Mg, and for **2**, M=Mg, N=Cu.

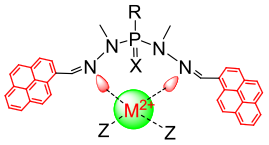

Scheme 2. Proposed interaction mode between ligand and the metal ion.

Fluorescence quantum yields in each case were determined by comparing the emission intensity of the sample with that of a fluorescence standard as anthracene (Φ_F=0.27±0.03).[33]

$$\Phi_U = \Phi_R(A_U/A_R)\left(n_U^2/n_R^2\right)$$

where A_U and A_R are the integrated area under the corrected fluorescence spectra for the sample and reference, n_U and n_R are the refractive indexes of the sample and reference, respectively. The stability constants[42] K_a was obtained from the fluorescence titration data. The linear fit of the fluorescence intensity data at a particular wavelength for 1:1 complexation was obtained by the use of following equation

$$I_F^0/\left(I_F - I_F^0\right) = [a/(b-a)][(1/K_a[M])]$$

where I_F^0 and I_F are the fluorescence intensity of the metal free ligand and the ML complex, respectively; [M] is the concentration of the metal ions added for complexation. The K_a is obtained as intercept/slope ratio from the plot of $I_F^0/(I_F-I_F^0)$ against $[M]^{-1}$.

4.3. General synthetic procedure

Quantitative amount of pyrene-1-carboxaldehyde (PyCHO) was dissolved in hot methanol (30 mL) and to it a methanol solution of corresponding phosphorus hydrazides was added dropwise. The reaction mixture was stirred at 50 °C for 12 h. A yellow precipitate was obtained. This was filtered, washed with hot methanol and then recrystallized from CH_2Cl_2/*n*-hexane mixture at 0 °C to get products.

4.3.1. Compound ***1***

PyCHO (0.230 g, 1.0 mmol); $Ph_2PO[N(CH_3)NH_2]$ (0.246 g, 1.0 mmol); **1** (0.357 g, 78%). Mp 180 °C. Crystals suitable for single-crystal X-ray diffraction were obtained after dissolving **1** in hot benzene and allowing it to remain at room temperature for three days. FTIR (KBr) (ν/cm^{-1}): 3044 m, 1583 s, 1436 s, 1306 s, 1223 s, 947 s, 826 s, 754 s. ^{1}H NMR (500 MHz, $CDCl_3$, 25 °C, TMS) δ (ppm)=3.45 (d, $-NCH_3$); ^3J ($^1H-^{31}P$)=6.0 Hz, 8.49 (s, 1H, CH=N), 7.49–8.15 (m, 21H, benzene and pyrene H). ^{13}C NMR (500 MHz, $CDCl_3$, 25 °C, TMS) δ (ppm)=30.17, 123.02, 124.95, 125.19, 125.44, 125.55, 126.06, 127.38, 127.83, 128.13, 128.32, 128.43, 130.63, 131.38, 131.44, 132.08, 132.36, 132.43. ^{31}P NMR (500 MHz, $CDCl_3$, 25 °C, TMS) δ (ppm)=32.95 (s). Anal. Calcd for $C_{30}H_{23}N_2OP$; ESI-HRMS: $[M+H]^+$=Calculated 459.1629, found 459.1629.

4.3.2. Compound ***2***

PyCHO (0.215 g, 0.92 mmol); $PhPO[N(CH_3)NH_2]_2$ (0.10 mg, 0.46 mmol); **2** (0.242 g, 80%). Mp 185 °C. Single-crystal X-ray

diffraction quality crystals of **2** and **2**·MeOH were obtained from its CH_2Cl_2/*n*-hexane and CH_2Cl_2/methanol solutions. FTIR (KBr) (ν/cm^{-1}): 3037 m, 1593 s, 1463 s, 1307 s, 1240 s, 958 s, 813 s, 749 s. ^1H NMR (400 MHz, $CDCl_3$, 25 °C, TMS) δ (ppm)=3.51 (d, –NCH_3); ^3J (^1H–^{31}P)=7.0 Hz, 8.58 (s, 1H, CH=N), 7.50–8.25 (m, 29H, pyrene H). ^{13}C NMR (500 MHz, $CDCl_3$, 25 °C, TMS) δ (ppm)=30.99, 122.94, 124.69, 124.93, 124.98, 125.13, 125.37, 125.46, 125.96, 127.38, 127.72, 128.05, 128.16, 128.23, 128.29, 130.61, 131.33, 131.40, 132.22, 133.30, 133.37, 136.04, 136.16. ^{31}P NMR (500 MHz, $CDCl_3$, 25 °C, TMS) δ (ppm)=26.620 (s). Anal. Calcd for $C_{42}H_{31}N_4OP$; ESI-HRMS: $[M+H]^+$=Calculated 639.2314, found 639.2312.

4.3.3. Compound **3**

PyCHO (0.460 g, 2.04 mmol); P(*S*)$[N(CH_3)NH_2]_3$ (0.135 g, 0.68 mmol); **3** (0.408 g, 72%). Mp 248 °C. Crystals suitable for single-crystal X-ray diffraction were obtained by dissolving **3** in hot acetonitrile/toluene and then allowing to slowly crystallizing at room temperature over a period of a week. FTIR (KBr) (ν/cm^{-1}): 3036 m, 2935 m, 1592 s, 1458 s, 1375 s, 1239 s, 951 s, 844 s, 761 s. ^1H NMR (400 MHz, $CDCl_3$, 25 °C, TMS) δ (ppm)=3.60 (d, –NCH_3); ^3J (^1H–^{31}P)=9.0 Hz, 8.65 (s, 1H, CH=N), 7.52–8.50 (m, 36H, pyrene H). ^{13}C NMR (500 MHz, $CDCl_3$, 25 °C, TMS) δ (ppm)=32.68, 122.84, 124.68, 124.86, 125.02, 125.06, 125.31, 125.83, 127.34, 127.49, 127.95, 128.33, 128.68, 130.59, 131.26, 136.02. ^{31}P NMR (500 MHz, $CDCl_3$, 25 °C, TMS) δ (ppm)=75.05 (s). Anal. Calcd for $C_{54}H_{39}N_6PS$; ESI-HRMS: $[M+H]^+$=Calculated 835.2773, found 835.2778.

4.3.4. Compound **4**

PyCHO (0.690 g, 3.00 mmol); $N_3P_3[N(CH_3)NH_2]_6$ (0.202 g, 0.50 mmol); **4** (0.57 g, 68%). Mp 210 °C. FTIR (KBr) (ν/cm^{-1}): 3037 m, 1593 s, 1460 s, 1378 s, 1265 s, 963 s, 844 s, 758 s. ^1H NMR (400 MHz, $CDCl_3$, 25 °C, TMS) δ (ppm)=3.76 (d, –NCH_3), 9.37 (s, 1H, CH=N), 6.35–7.78 (m, 72H, pyrene H). ^{13}C NMR (500 MHz, $CDCl_3$, 25 °C, TMS) δ (ppm)=32.84, 123.03, 124.57, 124.77, 125.00, 125.13, 125.74, 126.58, 126.85, 127.07, 127.20, 127.30, 127.42, 127.70, 128.17, 129.23, 130.64, 130.73, 130.85, 131.07, 131.31, 131.44. ^{31}P NMR (500 MHz, $CDCl_3$, 25 °C, TMS) δ (ppm)=19.406 (s). Anal. Calcd for $C_{108}H_{78}N_{15}P_3$; ESI-HRMS: $[M+H]^+$=Calculated 1678.5856, found 1678.6138.

Acknowledgements

We thank the Department of Science and Technology, India for financial support. V.C. is a Lalit Kapoor Chair Professor of Chemistry. V.C. is thankful to the Department of Science and Technology, for a J.C. Bose fellowship. This work is also supported by the *Bio-inorganic Chemistry Initiative*, DST, India.

Supplementary data

CCDC 718403–718406 (for compounds **1**, **2**, **2**·MeOH, and **3**) contain the supplementary crystallographic data for this paper. These data can be obtained free of charge from The Cambridge Crystallographic Data Centre via www.ccdc.cam.ac.uk/data_request/cif. Synthetic scheme of **1**–**4** and ESI-HRMS spectra of **1**–**4** are given. Supplementary data associated with this article can be found in the online version, at doi:10.1016/j.tet.2009.03.098.

References and notes

1. Uchiyama, S.; Kawai, N.; de Silva, A. P.; Iwai, K. *J. Am. Chem. Soc.* **2004**, *126*, 3032.
2. Shiraishi, Y.; Tokitoh, Y.; Hirai, T. *Org. Lett.* **2006**, *8*, 3841.
3. Jose, D. A.; Kumar, D. K.; Ganguly, B.; Das, A. *Org. Lett.* **2004**, *6*, 3445.
4. *Fluorescent Chemosensors for Ion and Molecule Recognition*; Desvergne, J. P., Czarnik, A. W., Eds.; Kluwer Academic: Dordrecht, The Netherlands, 1997.
5. de Silva, A. P.; Fox, D. B.; Huxley, A. J. M.; Moody, T. S. *Coord. Chem. Rev.* **2000**, *205*, 41.
6. Shiraishi, Y.; Ishizumi, K.; Nishimura, G.; Hirai, T. *J. Phys. Chem. B* **2007**, *111*, 8812.
7. (a) Martinez-Manez, R.; Sancenon, F. *Chem. Rev.* **2003**, *103*, 4419; (b) Ramachandram, B.; Saroja, G.; Sankaran, N. B.; Samanta, A. *J. Phys. Chem. B* **2000**, *104*, 11824.
8. de Silva, A. P.; McClenaghan, N. D.; McCoy, C. P. *Molecular Switches*; Wiley-VCH: New York, NY, 2000.
9. Czarnik, A. W. *Fluorescent Chemosensors for Ion and Molecular Recognition*; American Chemical Society: Washington, DC, 1992.
10. Hu, Z.; Qian, X.; Cui, J. *Org. Lett.* **2007**, *9*, 33.
11. Ravikumar, I.; Ahamed, B. N.; Ghosh, P. *Tetrahedron* **2007**, *63*, 12940.
12. Que, E. L.; Domaille, D. W.; Chang, C. J. *Chem. Rev.* **2008**, *108*, 1517.
13. Linder, M. C. *Biochemistry of Copper*; Plenum: New York, NY, 1991.
14. Xu, Z.; Xiao, Y.; Qian, X.; Cui, J.; Cui, D. *Org. Lett.* **2005**, *7*, 889.
15. Sumalekshmy, S.; Henary, M. M.; Siegel, N.; Lawson, P. V.; Wu, Y.; Schmidt, K.; Bredas, J.-L.; Perry, J. W.; Fahrni, C. J. *J. Am. Chem. Soc.* **2007**, *129*, 11888.
16. Chandrasekhar, V.; Azhakar, R.; Andavan, G. T. S.; Krishnan, V.; Zacchini, S.; Bickley, J. F.; Steiner, A.; Butcher, R. J.; Kögerler, P. *Inorg. Chem.* **2003**, *42*, 5989.
17. Chandrasekhar, V.; Pandian, B. M.; Boomishankar, R.; Steiner, A.; Vittal, J. J.; Houri, A.; Clećrac, R. *Inorg. Chem.* **2008**, *47*, 4918.
18. Sasaki, D. Y.; Shnek, D. R.; Pack, D. W.; Arnold, F. H. *Angew. Chem., Int. Ed. Engl.* **1995**, *34*, 905.
19. DeSantis, G.; Fabbrizzi, L.; Licchelli, M.; Poggi, A.; Taglietti, A. *Angew. Chem., Int. Ed.* **1996**, *35*, 202.
20. Bolleta, F.; Costa, I.; Fabbrizzi, L.; Licchelli, M.; Montalti, M.; Pallavicini, P.; Prodi, L.; Zaccheroni, N. *J. Chem. Soc., Dalton Trans.* **1999**, 1381.
21. Kim, S. K.; Lee, S. H.; Lee, J. Y.; Lee, J. Y.; Bartsch, R. A.; Kim, J. S. *J. Am. Chem. Soc.* **2004**, *126*, 16499.
22. Kim, H. J.; Park, S. Y.; Yoon, S.; Kim, J. S. *Tetrahedron* **2008**, *64*, 1294.
23. Kumar, S.; Singh, P.; Kaur, S. *Tetrahedron* **2007**, *63*, 11724.
24. Rurack, K.; Kollmannsberger, M.; Resch-Genger, U.; Daub, J. *J. Am. Chem. Soc.* **2000**, *122*, 968.
25. Park, S. M.; Kim, M. H.; Choe, J.-I.; No, K. T.; Chang, S.-K. *J. Org. Chem.* **2007**, *72*, 3550.
26. Birks, J. B. *Photophysics of Aromatic Molecules*; Wiley-Interscience: New York, NY, 1970.
27. (a) Vilkov, L. V.; Sadova, N. I.; Zilberg, I. Y. *Zh. Strukt. Khim.* **1967**, *8*, 528; (b) Wingerter, S.; Pfeiffer, M.; Murso, A.; Lustig, C.; Stey, T.; Chandrasekhar, V.; Stalke, D. *J. Am. Chem. Soc.* **2001**, *123*, 1381.
28. Baker, G. A.; Bright, F. V.; Pandey, S. *Chem. Educ.* **2001**, *6*, 223.
29. Waris, R.; Acree, W. E., Jr.; Street, K. W., Jr. *Analyst* **1988**, *113*, 1465.
30. Mazur, M.; Blanchard, G. J. *J. Phys. Chem. B* **2005**, *109*, 4076.
31. Behera, K.; Pandey, M. D.; Porel, M.; Pandey, S. *J. Chem. Phys.* **2007**, *127*, 184501.
32. Pandey, S.; Redden, R. A.; Fletcher, K. A.; Sasaki, D. Y.; Kaifer, A. E.; Baker, G. A. *Chem. Commun.* **2004**, 1318.
33. Dawson, W. R.; Windsor, M. W. *J. Phys. Chem.* **1968**, *72*, 3251.
34. Zeng, L.; Miller, E. W.; Pralle, A.; Isacoff, E. Y.; Chang, C. J. *J. Am. Chem. Soc.* **2006**, *128*, 10.
35. Sreejith, S.; Divya, K. P.; Ajayaghosh, A. *Chem. Commun.* **2008**, 2903.
36. Ray, D.; Bharadwaj, P. K. *Inorg. Chem.* **2008**, *47*, 2252.
37. Caballero, A.; Martinez, R.; Lloveras, V.; Ratera, I.; Vidal-Gancedo, J.; Wurst, K.; Tarraga, A.; Molina, P.; Veciana, J. *J. Am. Chem. Soc.* **2005**, *127*, 15666.
38. Nath, S.; Maitra, U. *Org. Lett.* **2006**, *8*, 3239; Kim, J. S.; Quang, D. T. *Chem. Rev.* **2007**, *107*, 3780.
39. Ji, H. F.; Brown, G. M.; Dabestani, R. *Chem. Commun.* **1999**, 609.
40. Leray, I.; O'Reilly, F.; Habib Jiwan, J.-L.; Soumillion, J.-P.; Valeur, B. *Chem. Commun.* **1999**, 795.
41. (a) *SMART and SAINT Software Reference Manuals, Version 6.45*; Bruker Analytical X-ray Systems: Madison, WI, 2003; (b) Sheldrick, G. M. *SADABS: A Software for Empirical Absorption Correction; Ver. 2.05*; University of Göttingen: Göttingen, Germany, 2002; (c) *SHELXTL Reference Manual, Ver. 6.1*; Bruker Analytical X-ray Systems: Madison, WI, 2000; (d) Sheldrick, G. M. *SHELXTL Ver. 6.12*; Bruker AXS: Madison, WI, 2001; (e) Bradenburg, K. *Diamond, Ver. 3.1d*; Crystal Impact GbR: Bonn, Germany, 2006.
42. Bag, B.; Bharadwaj, P. K. *J. Phys. Chem. B* **2005**, *109*, 4377.